Journal of Medicinal Chemistry

Article

pubs.acs.org/jmc

Discovery of Inhibitors To Block Interactions of HIV-1 Integrase with Human LEDGF/p75 via Structure-Based Virtual Screening and Bioassays

Guoping Hu,[†,#] Xi Li,[†,#] Xuan Zhang,[‡,#] Yaozong Li,[†] Lei Ma,[†] Liu-Meng Yang,[‡] Guixia Liu,[†] Weihua Li,[†] Jin Huang,*[,†] Xu Shen,[§] Lihong Hu,*[,§] Yong-Tang Zheng,*[,‡] and Yun Tang*[,†]

[†]Shanghai Key Laboratory of New Drug Design, School of Pharmacy, East China University of Science and Technology, 130 Meilong Road, Shanghai 200237, China

[‡]Key Laboratory of Animal Models and Human Diseases Mechanisms of Chinese Academy of Sciences and Yunnan, Kunming Institute of Zoology, Chinese Academy of Sciences, Kunming 650223, China

[§]Shanghai Research Center for the Modernization of Traditional Chinese Medicine, Shanghai Institute of Materia Medica, Chinese Academy of Sciences, Shanghai 201203, China

Supporting Information

ABSTRACT: This study aims to identify inhibitors that bind at the interface of HIV-1 integrase (IN) and human LEDGF/p75, which represents a novel target for anti-HIV therapy. To date, only a few such inhibitors have been reported. Here structure-based virtual screening was performed to search for the inhibitors from an *in-house* library of natural products and their derivatives. Among the 38 compounds selected by our strategy, 18 hits were discovered. The two most potent inhibitors showed IC_{50} values at 0.32 and 0.26 μM, respectively. Three compounds were subsequently selected for anti-HIV assays, among which (*E*)-3-(2-chlorophenyl)-1-(2,4-dihydroxyphenyl)prop-2-en-1-one (NPD170) showed the highest antiviral activity (EC_{50} = 1.81 μM). The antiviral mechanism of these compounds was further explored, and the results validated that the compounds interrupted the binding of transfected IN to endogenous LEDGF/p75. These findings could be helpful for anti-HIV drug discovery.

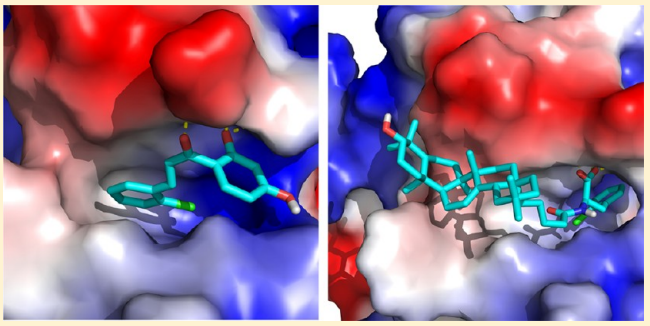

INTRODUCTION

HIV-1 integrase (IN) is a vital enzyme that catalyzes the insertion of proviral DNA into the host cell genome, which has been validated as a potential target because of its essential role in viral replication.[1] The integration process of IN consists of two steps: 3′-processing and strand transfer. Raltegravir was the first FDA-approved drug that targeted HIV-1 IN in the strand transfer (ST) step. However, raltegravir-resistant HIV emerged soon afterward.[2] Ceccherini-Silberstein et al. confirmed that primary and secondary integrase inhibitor (INI)-associated mutations are absent or extremely rare in INI-naive patients. Conversely, a few specific IN polymorphisms found in INI-naive patients increased their frequency in antiretroviral-failing patients and/or are associated with RT resistance mutations.[3] The emergence of viral strains resistant to clinically studied IN inhibitors demands the discovery of novel inhibitors that are structurally and mechanistically different.

Protein−protein interaction inhibitors (PPIIs) could allow the discovery of drugs that can conquer the HIV-resistance.[4] PPIIs are more resistant to spontaneous mutations at their binding sites. Several investigations have verified high conservation of amino acid residues within the contact interfaces compared with other regions of protein surfaces.[5−7] Indeed, mutation at the interface of a single subunit within the protein−protein complex may affect proper functional protein assembly, which is especially important for antiviral drug design.[8]

Cellular cofactors are important for the integration function of IN.[9] Among these cofactors, lens epithelial-cell-derived growth factor (LEDGF/p75) has been identified in complex with HIV-1 IN.[10,11] LEDGF/p75 is essential in IN nuclear distribution, without which the HIV-1 virus cannot replicate.[12,13] Therefore, disturbing or blocking IN−LEDGF/p75 interaction can prevent HIV-1 viral replication.[14−17] LEDGF/p75-mediated chromatin tethering is critical for viral integration and dependent on specific interactions between the integrase-binding domain (IBD) of LEDGF/p75 and the IN core domain.[14] Blocking IN−LEDGF/p75 interaction, a protein−protein interaction, provides a method of avoiding viral resistance and cross-resistance. Detailed interaction information between LEDGF/p75 IBD and the IN catalytic core domain

Received: August 23, 2012
Published: October 9, 2012

(CCD) is provided by the complex crystal structure (PDB code: 2B4J), which allows rational design of inhibitors that block the binding of LEDGF/p75 to IN. The LEDGF/p75 IBD inserts into a relatively small and deep cleft at the IN dimer interface during IN−LEDGF/p75 interaction.[15]

In a previous report, we identified that compound **D77** (see Chart 1), the first reported inhibitor to block IN−LEDGF/p75 interaction, can specifically act on the IN dimer interface.[18] A second inhibitor, C3003, was discovered by De Luca et al.[19] with an IC_{50} value of 35 μM, as tested by the AlphaScreen method. Subsequently, a series of compounds were developed based on compound C3003, among which compound CHIBA-3053 showed an IC_{50} value at 3.5 μM in the AlphaScreen assay (see Chart 1).[20] Recently, 2-(6-chloro-2-oxo-4-phenyl-1,2-dihydroquinolin-3-yl)acetic acid (compound **A**, see Chart 1) and 2-(6-chloro-2-methyl-4-phenylquinolin-3-yl)pentanoic acid (compound **B**, see Chart 1) were proven to bind to the LEDGF/p75 binding pocket of IN through complex crystal structures (PDB codes: 3LPT and 3LPU). These compounds showed IC_{50} values at 12 μM and 1 μM, respectively, through the AlphaScreen assay.[21] More recently, Tsiang et al.[22] from Gilead Sciences reported the most potent inhibitor **GS-B** (Chart 1), which has an IC_{50} value of 19 nM.

Chart 1. Representative Structures of Inhibitors Targeting IN−LEDGF/p75 Interaction

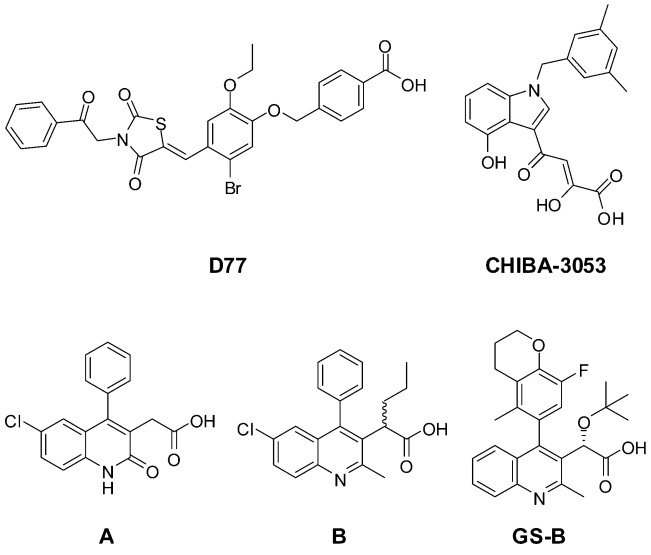

In the case of HIV-1 integrase, G140S/G148H and G148K are common mutations arising during raltegravir therapy. Christ et al.[23] demonstrated that inhibitors of IN−LEDGF/p75 interaction are not cross-resistant to INSTI-resistant mutants. Inhibitors of IN−LEDGF/p75 interaction are potent inhibitors of raltegravir-resistant virus strains. Compound **B** notably retained its full activity against all five raltegravir-resistant strains tested, underscoring its divergent mode of action.[21]

Natural products and their derivatives are always attractive sources of lead discovery due to their diverse structural types and thus may provide new perspectives for the design of IN−LEDGF/p75 interaction inhibitors.[24] In the present study, structure-based virtual screening (SBVS) was performed using an induced-fit model to discover inhibitors that target IN−LEDGF/p75 interaction from an *in-house* library of natural products and their derivatives. Among the 38 compounds selected by our strategy, 18 hits were identified as inhibitors through AlphaScreen bioassays. Three compounds were further tested in vitro for their anti-HIV-1 IN activity (EC_{50}) and cytotoxicity (CC_{50}) in cell-based assays against HIV-1 IN replication in acutely infected C8166 cells. In addition, the effects of the inhibitors on IN intracellular distribution were assayed on EGFP-fused IN-transfected 293T cells to identify their anti-HIV mechanism. The results provide a solid foundation for other investigations of inhibitors that target IN−LEDGF/p75 interaction.

RESULTS

Structure-Based Virtual Screening. Figure 1 illustrates the virtual screening process. The in-house library of natural products and derivatives in total contained 1430 compounds. Figure 2 shows that the distribution of molecular weight, AlogP, and number of H-bond donors and acceptors are rather wide, which indicate the diversity of the in-house natural products and derivatives library. All the compounds were docked against an induced-fit model of IN, named IFD_3LPT, which was developed from a crystal structure (PDB code: 3LPT). Although the resolution of 3LPT is fine (2.0 Å), it could not yield a reasonable binding mode for most known active compounds. Therefore, induced-fit docking was adopted to adjust the binding pocket based on 3LPT. We found that an induced-fit structure IFD_3LPT with a top IFD score could yield a reasonable binding mode for most known active compounds. Prior to database screening, it is crucial to test if a model or scoring function can distinguish active compounds from random compounds against a special target.[25] Model validation indicated that IFD_3LPT could yield ROC enrichment[26] higher than that of the two crystal structures, 3LPT and 3LPU, using both GlideScore and molecular mechanics-generalized Born surface area (MM-GB/SA) score (Figure S1 in Supporting Information). Therefore, IFD_3LPT was adopted as the virtual screening model in this study. The difference between induced-fit mode and 3LPT was compared and depicted in Figure S2 of Supporting Information. The main chain in the binding pocket did not show obvious changes, whereas the side chain of some key residues moved significantly. The hydrophilic subpocket seems shortened with the side-chain movement of residue Gln95 and Glu170. In contrast, the hydrophobic subpocket seems enlarged with the side-chain movement of residue Gln168 and Try132. After docking, 150 compounds with top GlideScores and another 150 compounds with top MM-GB/SA scores were stored separately for visual analysis after Glide standard precision (SP) docking and MM-GB/SA calculation. Visual inspection was

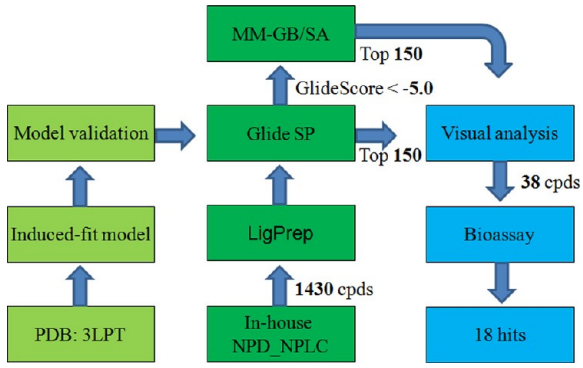

Figure 1. Schematic representation of hit discovery strategy.

dx.doi.org/10.1021/jm301226a | J. Med. Chem. 2012, 55, 10108−10117

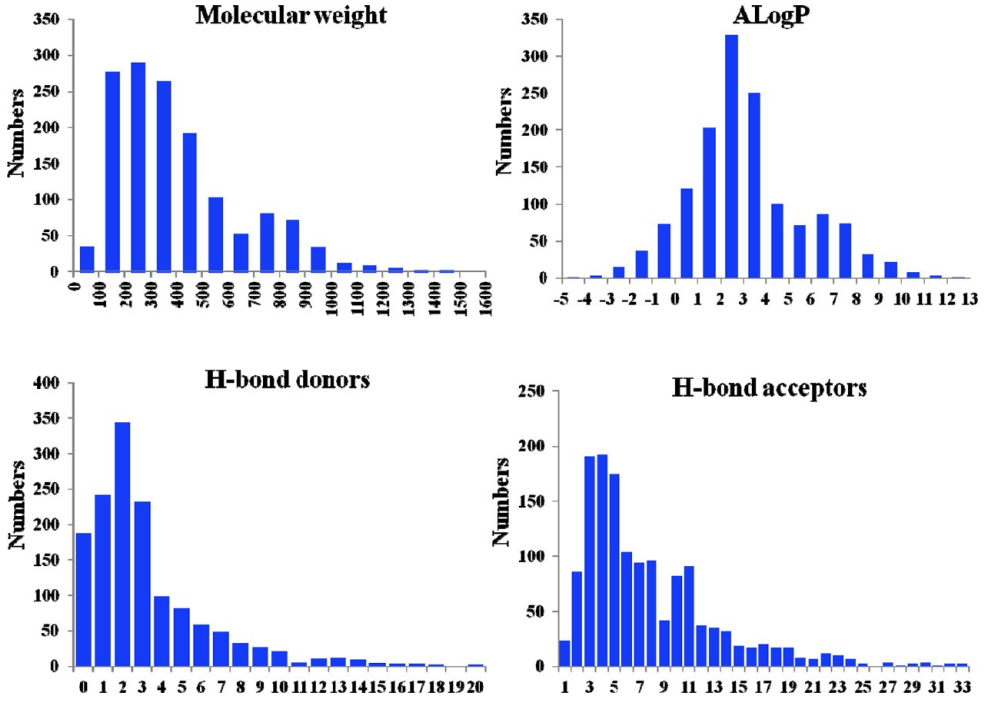

Figure 2. The distribution of molecular weight, AlogP, and number of H-bond donors and acceptors of the in-house natural products library.

adopted to check whether or not a compound created key interactions with protein. This step makes sure that the selected compounds have not only a higher score but also a reasonable binding mode. Finally, 38 compounds were selected for bioassays.

Bioassays at Molecular Level. The inhibitory activity of selected compounds was determined using the AlphaScreen assay to identify HIV-1 IN−LEDGF/p75 interaction inhibitors with potential values as novel regulators of HIV-1 integration (see the Experimental Section for details).[27] Results of the bioassays are presented in Table 1. Among the 38 tested compounds, significant inhibitory activities were detected on 18 compounds, with IC_{50} values ranging from 0.26 μM to 9.94 μM. In addition, original docking ranks prior to visual inspection and candidate selection are provided in Table S2 of the Supporting Information. In the present study, compound **A**, which was reported to block the IN−LEDGF/p75 interaction with an IC_{50} value at 12.2 μM by AlphaScreen assays,[21] was purchased and used as a positive control. Compound **A** showed an IC_{50} value at 11.65 μM in this study, approximating its previously reported value and thus confirming the accuracy and reliability of our bioassay. Five compounds even showed submicromolar inhibitory activity. The chemical structures of the 18 active compounds are shown in Chart 2. All active compounds can be categorized into four types, namely chalcone, oleanolic acid, rosmarinic acid, and salicylamide. These inhibitors are structurally diverse, but most of them belong to chalcone derivatives and oleanolic acid derivatives; only one inhibitor was categorized as rosmarinic acid, and one was categorized as salicylamide.

The inhibition curves of the six representative compounds in AlphaScreen assays are shown in Figure 3, which demonstrated an unambiguous dose-dependent effect. Inhibition curves of the other active compounds are shown in Figure S3 of the Supporting Information. Among these inhibitors, two chalcone derivatives, namely compound **7** and (*E*)-3-(2,3-dihydroxyphenyl)-1-(2,4,6-trihydroxyphenyl)prop-2-en-1-one

Table 1. Inhibitory Activities and cLogP and QPPCaco Values of 18 Active Compounds as well as Compound A

compound no.	IC_{50}[a] (μM)	cLogP[b]	QPPCaco[c]
1	3.67 ± 0.59	1.52	151.30
2	1.61 ± 0.22	2.18	216.74
3	6.21 ± 0.86	2.06	83.26
4	1.70 ± 0.26	1.42	64.83
5	3.78 ± 0.41	1.37	54.06
7	0.32 ± 0.06	3.27	470.68
8	1.75 ± 0.14	3.31	470.90
11	0.26 ± 0.05	1.36	29.93
13	3.84 ± 0.88	4.40	187.86
18	0.65 ± 0.05	9.39	86.69
19	4.56 ± 0.32	9.29	180.26
20	1.26 ± 0.11	9.29	108.43
21	3.22 ± 0.06	9.15	129.05
22	9.94 ± 3.08	6.12	10.63
23	1.14 ± 0.08	8.03	20.63
24	5.51 ± 0.97	7.57	20.45
25	0.70 ± 0.07	8.84	595.71
37	0.55 ± 0.14	1.15	1.65
compound **A**	11.65 ± 1.12	3.10	89.09

[a]Concentration required inhibiting the HIV-1 IN−LEDGF/p75 interaction by 50%. [b]cLogP values of compounds were calculated with QikProp. [c]QPPCaco values of compounds were calculated with QikProp.

(NPD177), showed the most potent activities, with IC_{50} values at 0.32 and 0.26 μM, respectively. Rosmarinic acid (NPLC0542) and two oleanolic acid derivatives, 3-(2-chlorophenyl)-2-(5-((4a*R*,6a*S*,6b*R*,10*S*,12a*R*)-10-hydroxy-2,2,6a,6b,9,9,12a-heptamethyl-1,2,3,4,4a,5,6,6a,6b,7,8,8a,9,-10,11,12,12a,12b,13,14b-icosahydropicen-4a-yl)pentanamido)-propanoic acid (NPD268) and (4a*S*,6a*S*,6b*R*,10*S*,12a*R*)-10-(benzyloxy)-2,2,6a,6b,9,9,12a-heptamethyl-1,2,3,4,4a,5,6,6a,6b,7,8,8a,9,10,11,12,12a,12b,13,14b-icosahy-

dx.doi.org/10.1021/jm301226a | *J. Med. Chem.* 2012, 55, 10108−10117

Chart 2. Chemical Structures of Active Compounds

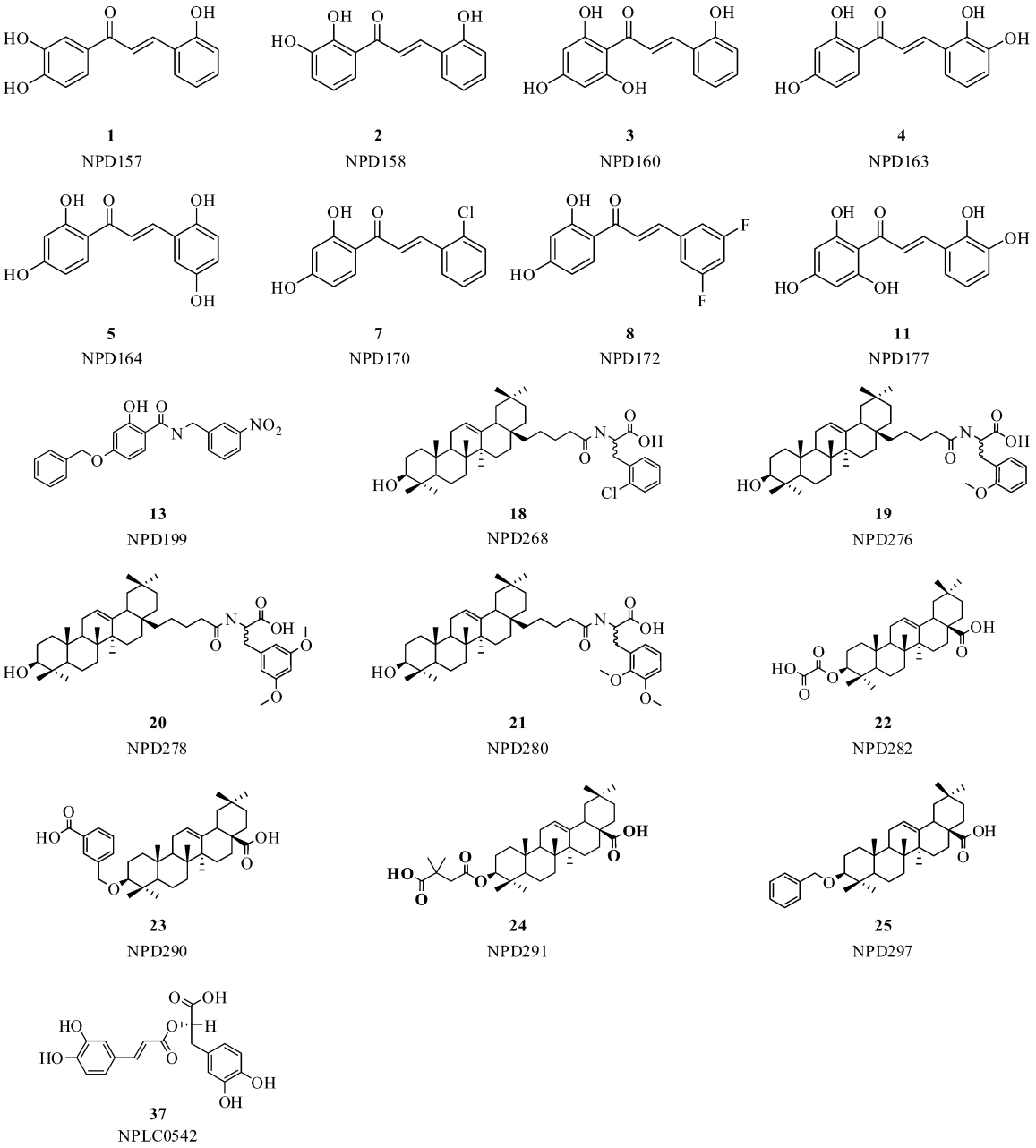

dropicene-4a-carboxylic acid (NPD297), showed relatively potent activities, with IC_{50} values at 0.55, 0.65, and 0.70 μM, respectively. The salicylic-type compound, 4-(benzyloxy)-2-hydroxy-*N*-(3-nitrobenzyl)benzamide (NPD199), showed low micromolar activity. Some compounds did not display a normal sigmoidal curve which might due to the comparably narrow range of concentration. The different slopes might have relationships to the different characteristics of compounds.

Anti-HIV Activity and Cellular Toxicity. Following the remarkable activities of several inhibitors toward isolated HIV-IN and LEDGF/p75, we further investigated the antiviral activities of the three most promising inhibitors, compounds 7, **11** (NPD177), and **18** (NPD268), on HIV-1_{IIIB}-infected C8166 cells. The cytopathic effect (CPE) was measured by counting the number of syncytia under microscope, and the percentage inhibition of syncytia formation was calculated. 3′-Azido-3′-deoxythymidine (AZT) was used as a positive control. Cellular toxicity of compounds on C8166 cells was assessed by the 3-(4,5-dimethylthiazol-2-yl)-2,5-diphenyltetrazolium bromide (MTT) method (see Experimental Section). When these assays were utilized, the EC_{50} and CC_{50} values for compounds 7, **11**, and **18** were determined from the dose−response curve (Figure 4A,B). Table 2 summarizes the antiviral testing results. All three compounds exhibited potent anti-HIV-1 activity, with EC_{50} values at 1.81, 26.92, and 36.59 μM, respectively, and a therapeutic index (TI) of 4.88, 3.76, and 2.12, respectively. Comparably narrow TIs indicate the necessity of further structural optimization to develop therapeutic drugs.

Effect of Inhibitors on EGFP−IN Intracellular Distribution. EGFP-fused IN was transfected into 293T cells to identify the effects of the compounds on IN intracellular distribution. Transient expression of EGFP−IN resulted in a significant nuclear localization (Figure 5A). Compound **D77** was used as a positive control.[18] Figure 5B−E shows that the

dx.doi.org/10.1021/jm301226a | J. Med. Chem. 2012, 55, 10108−10117

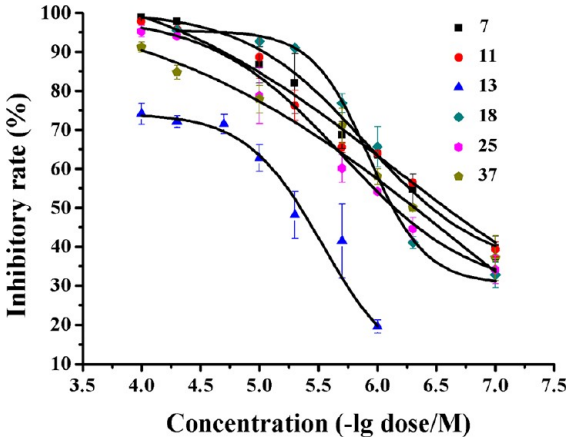

Figure 3. Dose−response curves of six representative IN−LEDGF/p75 interaction inhibitors in the AlphaScreen assay. Compound labels are listed on the right. The data of the AlphaScreen assay resulted from at least two independent experiments. Error bars represent the standard error of the mean (SEM).

addition of **D77** (83.83 μM), **7** (36.40 μM), **11** (86.73 μM), and **18** (36.00 μM) affected the nuclear accumulation of EGFP−IN. Compared with EGFP−IN-transfected cells untreated with **D77**, EGFP−IN appeared diffusely distributed in the cytoplasm and almost no fluorescence could be observed in the nucleus. Therefore, compounds **7**, **11**, and **18** may disrupt IN nuclear distribution by interrupting the binding of transfected IN to endogenous LEDGF/p75.

DISCUSSION

Confirmation of Binding Site. LEDGF/p75 is essential in IN nuclear distribution and chromatin tethering, critical for viral integration, and dependent on specific interactions between the IBD of LEDGF/p75 and the IN core domain. The HIV-1 virus cannot replicate without LEDGF/p75. Therefore, IN−LEDGF/p75 interaction represents a critical target for anti-HIV therapy and may provide a new approach to avoid viral resistance and cross-resistance. In the present study, 18 compounds were identified to block IN−LEDGF/p75 interaction through the AlphaScreen bioassay. Three representative inhibitors showed potent anti-HIV activity, and the effects of these compounds on IN intracellular distribution further demonstrated that they block the IN nuclear distribution by interrupting the binding of transfected IN to endogenous LEDGF/p75.

Table 2. Anti-HIV-1 Activity of Three Selected Compounds as well as AZT on C8166 Cells in Vitro

compound no.	EC_{50}[a] (μM)	CC_{50}[b] (μM)	TI[c]
7	1.81 ± 0.14	8.83 ± 0.87	4.88
11	29.62 ± 0.56	111.33 ± 3.18	3.76
18	36.59 ± 8.85	77.51 ± 1.87	2.12
AZT[d]	0.0087 ± 0.0004	4107.39 ± 616.18	473128.45

[a]EC_{50} (50% effective concentration), concentration of test compound that reduces syncytia formation by 50%. [b]CC_{50} (50% cytotoxic concentration), concentration of test compound that causes 50% reduction in total C8166 cell number. [c]TI is a ratio of the CC_{50} value/EC_{50} value. [d]AZT was used as a positive control.

Table 1 shows that compound **11** exhibits inhibitory activity higher than that of compound **7** in the AlphaScreen assay but yields lower anti-HIV activity. This result may be attributed to the different permeability characteristics of the two compounds. Compound **11** has five phenolic hydroxyl groups, whereas compound **7** has two. The calculated log *P* (cLogP) of compounds **7** and **11** are 3.27 and 1.36, respectively. A higher log *P* value is favorable for penetration into C8166 cells. In addition, Caco-2 cell permeability of these two compounds were predicted using QikProp.[28] Caco-2 cells are a model for the gut−blood barrier. QikProp predictions are for nonactive transport. The predicted Caco-2 cell permeability values for compounds **7** and **11** are 470.68 and 29.93, respectively, which indicated clearly that compound **7** has better cell permeability than compound **11**.

Structure−Activity Analysis. A set of chalcone and oleanolic acid derivatives were selected and identified as inhibitors; therefore, the preliminary structure−activity relationship could be analyzed. For chalcone derivatives, the aromatic ring adjacent to the carbonyl group was named as A-ring and another aromatic ring was named as B-ring. Obviously, the inhibitory activities of chalcone derivatives are governed to a greater extent by the hydroxyl substituents on the A- and B-rings, and the most active compound is substituted with five hydroxyl groups (compound **11**, IC_{50} = 0.26 μM). Comparing the active compound (*E*)-3-(3,5-difluorophenyl)-1-(2,4-dihydroxyphenyl)prop-2-en-1-one (NPD172) with the inactive compound (*E*)-1-(4-(benzyloxy)-2-hydroxyphenyl)-3- (3,5-difluorophenyl)prop-2-en-1-one (NPD182, Table S4), we found that the *p*-hydroxyl on ring A is needed for activity. Through the comparison among active compounds (*E*)-3-(2,3-dihydroxyphenyl)-1-(2,4-dihydroxyphenyl)prop-2-en-1-one

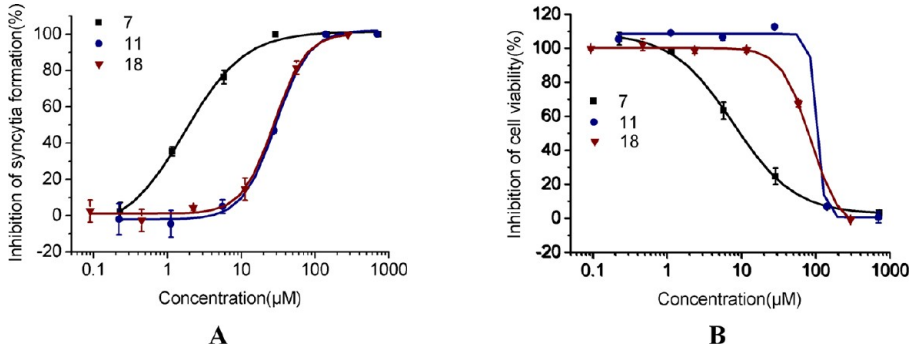

Figure 4. Dose−response curves of compounds **7**, **11**, and **18**. (A) The EC_{50} of compounds were determined utilizing the C8166 cell line infected with HIV-1_{IIIB}. (B) The CC_{50} of compounds was determined utilizing the MTT-based cytotoxicity assay. The data of anti-HIV activities resulted from at least two independent experiments. Error bars represent the standard error of the mean (SEM).

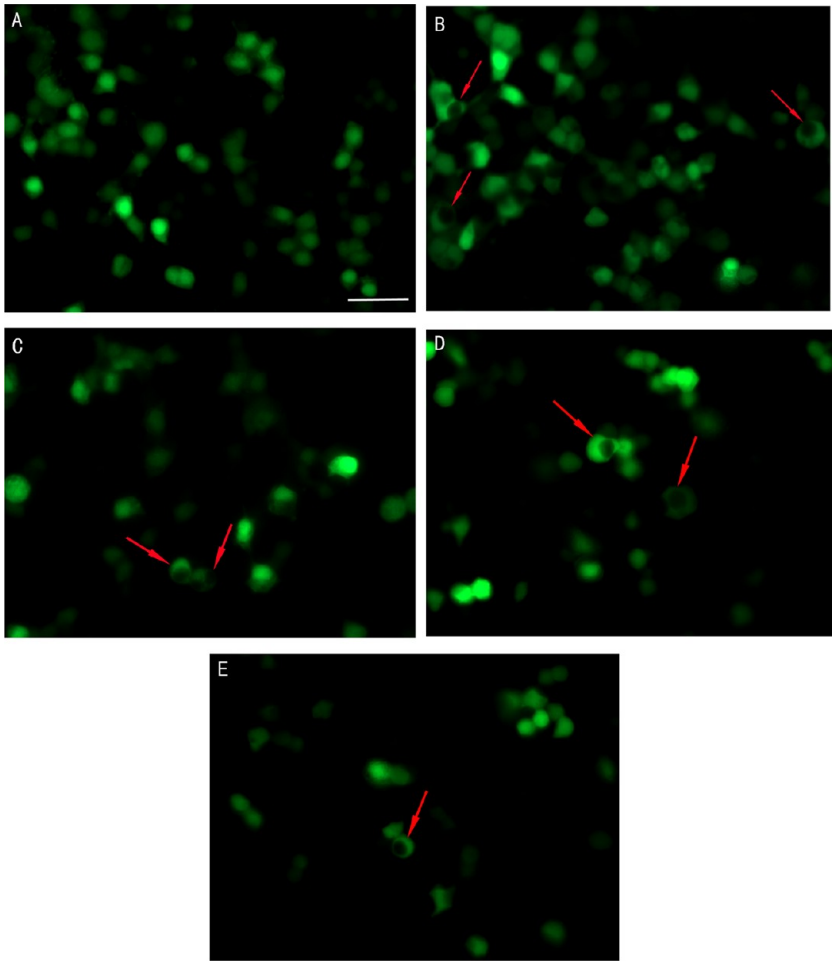

Figure 5. Effects of inhibitors on EGFP−IN nuclear distribution in 293T cells transformed with pEGFP−IN plasmid. (A) Without inhibitor, EGFP−IN was mainly distributed in the nucleus; (B) treated with 83.83 μM of **D77**, EGFP−IN was mainly distributed in the cytoplasm; (C) treated with 36.40 μM of compound **7**; (D) treated with 86.73 μM of compound **11**; (E) treated with 36.00 μM of compound **18**. Red arrowheads show the EGFP−IN distribution. The scale bar is 50 μm.

(NPD163), compound **11**, and the inactive compound (*E*)-1-(2,4-dihydroxyphenyl)-3- (2,6-dihydroxyphenyl)prop-2-en-1-one (NPD165, Table S4), we found that an additional *o*-hydroxyl group on the A-ring is favorable, whereas an additional *o*-hydroxyl group on the B-ring is unfavorable. With a chlorine group substituted on its B-ring, compound **7** shows the second highest inhibitory activity (IC_{50} = 0.32 μM), indicating that the hydroxyl substituents on the A-ring are more favorable and that the B-ring can be substituted by hydrophobic groups. As shown in Figure S1 of Supporting Information, model validation has been carried out using an external data set, which indicated that the induced-fit model could yield higher enrichment of active compounds under either GlideScore or MM-GBSA score. In this study, chalcone-type compounds were selected according to their higher GlideScore, because their polyhydroxyl ring can form hydrogen bonds with polar residues. Nevertheless, chalcone is a kind of α,β-unsaturated carbonyl compound and has the potential to act as a Michael acceptor. Therefore, chalcone should be carefully considered in the next study.

For oleanolic acid derivatives, the inhibitory activities are tolerant to both the inserted linker between the carboxyl group and ring and different substitutents on the hydroxyl group. Four oleanolic acid derivatives including compound **18**, 2-(5-((4a*R*,6a*S*,6b*R*,10*S*,12a*R*)-10-hydroxy-2,2,6a,6b,9,9,12a-heptamethyl-1,2,3,4,4a,5,6, 6a,6b,7,8,8a,9,10,11,12,12a,12b,13,14b-icosahydropicen-4a-yl)pentanamido)-3-(2-methoxyphenyl)-propanoic acid (NPD276), 3-(3,5-dimethoxyphenyl)-2-(5-((4a*R*,6a*S*,6b*R*,10*S*,12a*R*)-10-hydroxy-2,2,6a,6b,9,9,12a-heptamethyl-1,2,3,4,4a,5,6,6a,6b,7,8,8a,9,10,11,12,12a,12b,13,14b-icosahydropicen-4a-yl)pentanamido)propanoic acid (NPD278), and 3-(2,3-dimethoxyphenyl)-2-(5-((4a*R*,6a*S*,6b*R*,10*S*,12a*R*)-10-hydroxy-2,2,6a,6b,9,9,12a-heptamethyl-1,2,3,4,4a,5,6,6a,6b,7,8,8a,9,10,11,12,12a,12b,13,14b-icosahydropicen-4a-yl)pentanamido)propanoic acid (NPD280) are structurally similar and differ only in terms of the substituted groups on their aromatic rings; all four oleanolic acid derivatives are racemic with respect to the α-carbon of the carboxylate group. Among the four derivatives, compound **18** yields the highest inhibitory activity, with chlorine substituted on the ortho-position. Substitution of a methoxyl group on the same position leads to a decrease in inhibitory activity. Docking results of the two chiral isomers of the four compounds indicated that the *R*-configuration might be favorable for their activity. Compared with the inactive *R*-configuration compound (*R*)-2-((4a*S*,6a*S*, 6b*R*,8a*S*,10*S*,12a*R*,12b*S*,14b*S*)-10-hydroxy-2,2,6a,6b,9,9,12a-heptamethyl-1,2,3,4,4a,5,6,6a,6b,7,8,8a,9,-10,11,12,12a,12b,13,14b-icosahydropicene-4a-carboxamido)-3-phenylpropanoic acid (NPLC0783, Table S4), the linker between the pentacyclic system and amide seems necessary for activity.

dx.doi.org/10.1021/jm301226a | *J. Med. Chem.* 2012, 55, 10108−10117

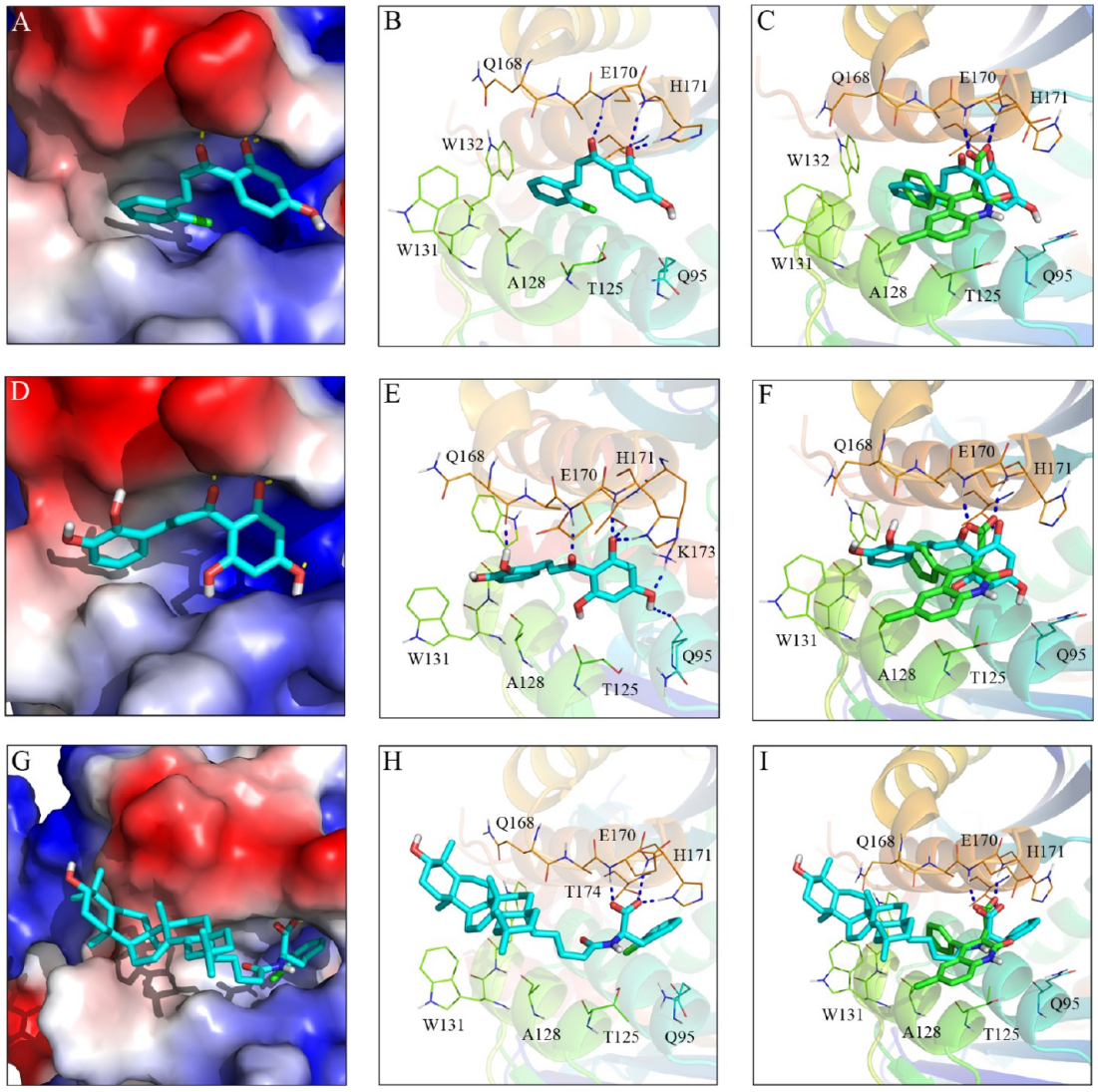

Figure 6. Putative binding modes of compounds **7** (A, B), **11** (D, E), and **18** (G, H) via IFD. The binding pocket of the enzyme was illustrated as (A, D, G) solvent-accessible surface colored by electrostatic potentials and (B, E, H) thin lines for key residues and light ribbon for others. Ligands are colored in cyan. Blue dashed lines represent H-bonding interactions between the ligand and receptor. The binding modes of the three inhibitors were superposed to compound **A** of crystal structure 3LPT (C, F, and I). These figures were prepared using PyMOL (http://www.pymol.org/).

Another four oleanolic acid derivatives including (4a*S*,6a*S*,6b*R*,10*S*,12a*R*)-10-(carboxycarbonyloxy)-2,2,6a,6b,9,9,12a-heptamethyl-1,2,3,4,4a,5,6,6a,6b,7,8,8a,9,-10,11,12,12a,12b,13,14b-icosahydropicene-4a-carboxylic acid (NPD282), (4a*S*,6a*S*,6b*R*,10*S*,12a*R*)-10-(3-carboxybenzyloxy)-2,2,6a,6b,9,9,12a-heptamethyl-1,2,3,4,4a,5,6,6a,6b,7,8,8a,9,10,11,12,12a,12b,13,14b-icosahydropicene-4a-carboxylic acid (NPD290), (4a*S*,6a*S*,6b*R*,10-*S*,12a*R*)-10-(3-carboxy-3-methylbutanoyloxy)-2,2,6a,6b,9,9,12a-heptamethyl-1,2,3,4,4a,5,6,6a,6b,7,8,8a,9,-10,11,12,12a,12b,13,14b-icosahydropicene-4a-carboxylic acid (NPD291), and compound **25** (NPD297) have different substituted groups on the hydroxyl group. Among them, compound **25** has the highest inhibitory activity, indicating that hydrophobic groups are favorable at this position. Table 1 shows that the calculated cLogP of all oleanolic acid derivatives range from 6.12 to 9.81, indicating that further optimization is necessary to develop druglike compounds.

With an extended structure, the oleanolic acid derivatives possess characteristics of PPIIs. Higher hydrophobic content and an extended interaction surface are favorable to disturb the protein−protein interaction. However, compared with oleanolic acid, chalcone has a very simple structure. The most potent chalcone derivative, compound **11**, can disturb protein−protein interaction at the submicromolar level. This result supports the idea that for some protein−protein interfaces, the affinity of the interaction is governed by a small, well-defined, compact subarea of a larger interface, namely the "hot spots".[8] Interestingly, while chalcone-type compounds have GlideScores higher than those of oleanolic acid-type compounds, oleanolic acid-type compounds have higher MM-GB/SA scores (Table S2 of Supporting Information). All of the selected chalcone derivatives contain at least one polyhydroxyl aromatic ring, which may form more polar interactions with the appropriate receptors and yield higher GlideScores. In contrast, the oleanolic acid derivatives contain a pentacyclic triterpene core structure that lacks polar interactions with receptors. However, larger oleanolic acid derivatives can form more nonpolar interactions and yield higher MM-GB/SA scores. This

dx.doi.org/10.1021/jm301226a | *J. Med. Chem.* 2012, 55, 10108−10117

observation provides new data and knowledge for future screening and structural modification.

Binding Mode Analysis. IN is recognized by LEDGF/p75 through the following two key features: the specific backbone conformation of residues 168−171, which can form a hydrogen-bond network with IBD, and a hydrophobic patch that accommodates the side-chain residues of LEDGF/p75, namely Ile365, Phe406, and Val408.[29] The Asp366 of LEDGF/p75 forms a bidentate hydrogen bond with the main-chain amides of the IN residues, Glu170 and His171, in chain A. Ile365 projects into a hydrophobic pocket formed by Thr174 and Met178 in chain A as well as Leu102, Ala128, Ala129, and Trp132 in chain B. Using GRID molecular interaction fields, De Luca et al.[20] explored a hydrophobic region for ligand binding located near Trp131 in the B chain. Site mutagenetic studies also highlighted the role of Trp131.[18,30]

Plausible binding modes of three representative compounds via induced-fit docking (IFD) are shown in Figure 6. The docking poses of compounds **7** and **11** reveal that the carbonyl group and the *o*-hydroxyl group of the A-ring form a hydrogen bond network with the main-chain amides of Glu170 and His171 and the side chain of His171 and Thr174 in chain A. Compound **11** forms additional hydrogen bonds with the side chain of Lys173 in chain A and the main chain of Gln95 in chain B. In particular, the phenolic hydroxyl group of the B-ring of compound **11** forms a hydrogen bond with the backbone of Gln168. The B-ring of both compounds is located in the hydrophobic pocket. The docking pose of compound **18** reveals that the carboxyl group forms hydrogen bonding interactions with the main-chain amide of Glu170 and His171 and the side chain of His171 and Thr174 in chain A. The triterpenoid skeleton of compound **18** occupies the hydrophobic pocket. The superposition results indicated that the binding modes of the three inhibitors are very similar to that of the known inhibitor in the crystal structure. Especially, they all formed the characteristic bidentate hydrogen bond with the main-chain amide of Glu170 and His171.

■ CONCLUSION

In the study, an in-house library containing natural products and their derivatives was virtually screened against an induced-fit model of HIV-1 integrase for new inhibitors to block IN−LEDGF/p75 interaction. Eighteen of the thirty-eight tested compounds were discovered as potent inhibitors via AlphaScreen assays, indicating the high success rate of this approach. The most potent compound **11** showed an IC_{50} value of 0.26 μM. Three compounds demonstrated significant anti-HIV activities. In particular, compound **7**, which showed the highest anti-HIV activity, had an EC_{50} value of 1.81 μM and a TI of 4.88. The three compounds also blocked IN nuclear distribution by interrupting the binding of transfected IN to endogenous LEDGF/p75. Compared with currently known active compounds, these newly identified inhibitors have significant potential for further development.

■ EXPERIMENTAL SECTION

Protein Preparation. The crystal structure of HIV-1 IN CCD dimer complexed with compound **A** (PDB code: 3LPT) was used as a starting point to generate an induced-fit model of the enzyme. Compounds **A**, **B**, CX05045,[23] and CHIBA-3053 were employed in this process. IFD workflow of Maestro 9.0 was utilized with Prime 2.1[31] and Glide 5.5[32] to adjust the receptor structure, especially in the binding pocket. All docking calculations were run in the "Standard Precision" (SP) mode of Glide, the center of the grid box was set to that of the ligand, and the box size was set to auto. All other parameters were left at default settings. All docked structures were automatically ranked according to their IFD score. The induced-fit structure with top IFD score was adopted in following virtual screening (named as IFD_3LPT).

Ligand Preparation. All compounds in the in-house library were prepared with Ligprep 2.3.[33] During this process, the OPLS_2005 force field was chosen and the possible ionization states of each compound at the pH range of 5.0−9.0 were generated. The cLogP and QPPCaco values of compounds were calculated with QikProp.[28]

Glide Docking and MM-GB/SA Rescoring. The prepared small molecules were docked against IFD_3LPT using Glide SP with default settings.[34] After docking, the ligand−receptor binding free energy for each ligand was calculated using MM-GB/SA provided by the "Prime MM-GBSA" module.[31] Only the top ranked molecules (GlideScore < −5.0) were submitted for MM-GB/SA calculation. All protein atoms were frozen, and only ligand structures were relaxed during MM-GB/SA calculation. The ligand strain energies were also calculated.[35]

Chemistry. All test compounds were selected from the in-house library containing natural products and their derivatives. The syntheses of these compounds have been reported previously.[36,37] The structures and purities of the 18 inhibitors were determined by ^{1}H NMR, mass spectra, and HPLC analysis (Table S3 of Supporting Information). ^{1}H NMR spectra were measured on a Bruker AM-400 or a Varian Mercury-VX300 spectrometer. ESI-MS was run on a Bruker Esquire 3000 plus spectrometer in MeOH, and HR-ESI-MS was run on a Bruker Atex III spectrometer in MeOH. HPLC analysis used a Waters 2695 Alliance LC System with a KR100-C18 Kromasil column (150 × 4.6 mm, 5 μm particle size), flow rate 1.0 mL/min; UV wavelength, 210 or 254 nm. All tested compounds have a purity ≥95%.

AlphaScreen Assay. The inhibitory activities against the IN−LEDGF/p75 interaction were tested using AlphaScreen assays as described by Hou et al.[27] The HIV-1 IN CCD was expressed and purified as described by Jenkins et al.[38] The IBD of LEDGF/p75 (residues 347−442) containing a GST tag was prepared as previously reported.[18] Reactions were performed in a 25 μL final volume in 384-well ProxiPlates (PerkinElmer). The buffer was composed of 25 mM HEPES, pH 7.3, 150 mM NaCl, 2 mM $MgCl_2$, 1 mM DTT, and 0.1% BSA. The His_6-tagged HIV IN CCD was added to a final concentration of 40 nM and incubated with test compounds at varying concentrations (0.1−100 μM) and room temperature for 30 min. Subsequently, the remaining components containing a GST-tagged LEDGF/p75 IBD (final concentration, 40 nM), nickel chelate acceptor beads (final concentration, 8 μg/mL), and glutathione donor beads (final concentration, 8 μg/mL) were added to the well. Proteins and beads were incubated at room temperature for 2 h. The incubation was performed in the dark to avoid direct light exposure. The plates were measured with an EnVision Multilabel Plate Reader (PekinElmer), with the final emission ranging from 520 to 620 nm.

MTT-Based Cytotoxicity Assay. Cellular toxicity of compounds on C8166 cells was assessed by MTT method as described previously.[39] Briefly, cells were seeded on 96-well microtiter plate in the absence or presence of various concentrations of compounds in triplicate and incubated at 37 °C in a humid atmosphere of 5% CO_2 for 3 d. The supernatants were discarded, MTT reagent (12.1 mM in PBS) was added to each well and then incubated for 4 h, and 100 μL of 50% *N*,*N*-dimethylformamide (DMF)−20% SDS was added. After the formazan was dissolved completely, the plates were read on a Bio-Tek Elx 800 ELISA reader at 595/630 nm. The cytotoxic concentration that caused the reduction of viable C8166 cells by 50% (CC_{50}) was determined from the dose−response curve.

Anti-HIV Activity Assay. C8166 cells (4×10^4 cells per well), infected with HIV-1_{IIIB} at a multiplicity of infection (M.O.I. 0.15), were seeded on a 96-well plate in the absence or presence of various gradient concentrations of compounds in triplicate. The final volume per well was 200 μL. After 3 d of culture, the CPE was measured by counting the number of syncytia under microscope. Percentage inhibition of syncytia formation was calculated, and 50% effective concentration (EC_{50}) was calculated from the dose−response curve.

AZT (Sigma) was used as a positive control. Therapeutic index (TI) = CC_{50}/EC_{50}. The data of anti-HIV activities resulted from at least two independent experiments, and the compounds were completely dissolved at the concentrations used in the experiment.

EGFP−IN Intracellular Distribution Assay. 293T cells were cultured and maintained in Dulbecco's modified Eagle's medium (DMEM) supplemented with 10% fetal bovine serum (FBS), 144.36 μM G418, and 100 U/mL streptomycin−penicillin (Invitrogen) at 37 °C in a 5% CO_2 incubator. Twenty-four hours before transfection, 293T cells (1 × 105/well) were seeded onto a clear 96-well plate in DMEM containing 10% FBS. 293T cells were transfected by EGFP−C-IN expression plasmid (The Chinese University of Hong Kong) using Lipofectamine 2000 reagent (Invitrogen). The medium was removed 5 h after transfection. Fresh medium containing compounds was added at different concentrations. Twenty-four hours after transfection, cells were fixed with 4% paraformaldehyde in PBS at room temperature for 15 min. Cell imaging was performed with a Leica DMI4000 microscope. **D77** was used as a positive control.

■ ASSOCIATED CONTENT

Ⓢ Supporting Information

Model validation and docking ranks of active compounds and concentration−inhibition curves; ^{1}H NMR, mass spectra, and HPLC data of active compounds. This material is available free of charge via the Internet at http://pubs.acs.org.

Accession Codes

2B4J, 3LPT, 3LPU.

■ AUTHOR INFORMATION

Corresponding Author

*(For J.H. and Y.T.) Tel.: +86-21-6425-1052, fax: +86-21-6425-3651, e-mail: huangjin@ecust.edu.cn; ytang234@ecust.edu.cn. (For L.H.) Tel.: +86-21-2023-1965, e-mail: simmhulh@mail.shcnc.ac.cn. (For Y.-T.Z.) Tel.: +86-871-519-5684, fax: +86-871-519-5684, e-mail: zhengyt@mail.kiz.ac.cn.

Author Contributions

#These authors contributed equally to this work.

Notes

The authors declare no competing financial interest.

■ ACKNOWLEDGMENTS

This work was supported by the Program for New Century Excellent Talents in University (Grant NCET-08-0774), the Fundamental Research Funds for the Central Universities (Grant WY1113007), the Shanghai Committee of Science and Technology (Grant 11DZ2260600), the National Natural Science Foundation of China (grants 30925040 and 81102483), and the Key Scientific and Technological Program of China (grants 2012ZX10001-006 and 2012ZX09103-101-022). The cDNA coding for HIV IN catalytic core domain (residues 50−212) including the F185K solubilizing-mutation was a gift from Prof. Robert Craigie (National Institutes of Health, Bethesda, MD). The full-length plasmid pCPNat p75 was kindly provided by Prof. Zeger Debyser (Katholieke Universiteit Leuven, Belgium).

■ ABBREVIATIONS USED

IN, integrase; CCD, catalytic core domain; IBD, integrase binding domain; VS, virtual screening; MM-GB/SA, molecular mechanics-generalized Born surface area; LEDGF, lens epithelial-cell-derived growth factor; MTT, 3-(4,5-dimethylthiazol-2-yl)-2,5-diphenyltetrazolium bromide; PPIIs, protein−protein interaction inhibitors; ROC, receiver operating characteristics; IFD, induced-fit docking; CPE, cytopathic effect; AZT, 3′-azido-3′-deoxythymidine; TI, therapeutic index; cLogP, calculated log *P*; EGFP, enhanced green protein; DTT, dithiothreitol; SDS, sodium dodecyl sulfate; BSA, bovine serum albumin; PBS, phosphate-buffered saline; MOI, multiplicity of infection; CPE, cytopathic effect; PDB, Protein Data Bank

■ REFERENCES

(1) Anthony, N. J. HIV-1 integrase: A target for new AIDS chemotherapeutics. *Curr. Top. Med. Chem.* **2004**, *4*, 979−990.

(2) Malet, I.; Delelis, O.; Valantin, M. A.; Montes, B.; Soulie, C.; Wirden, M.; Tchertanov, L.; Peytavin, G.; Reynes, J.; Mouscadet, J. F.; Katlama, C.; Calvez, V.; Marcelin, A. G. Mutations associated with failure of raltegravir treatment affect integrase sensitivity to the inhibitor in vitro. *Antimicrob. Agents Chemother.* **2008**, *52*, 1351−1358.

(3) Ceccherini-Silberstein, F.; Malet, I.; Fabeni, L.; Dimonte, S.; Svicher, V.; D'Arrigo, R.; Artese, A.; Costa, G.; Bono, S.; Alcaro, S.; Monforte, A.; Katlama, C.; Calvez, V.; Antinori, A.; Marcelin, A. G.; Perno, C. F. Specific HIV-1 integrase polymorphisms change their prevalence in untreated versus antiretroviral-treated HIV-1-infected patients, all naive to integrase inhibitors. *J. Antimicrob. Chemother.* **2010**, *65*, 2305−2318.

(4) Al-Mawsawi, L. Q.; Neamati, N. Allosteric inhibitor development targeting HIV-1 integrase. *ChemMedChem* **2011**, *6*, 228−241.

(5) Arkin, M. R.; Wells, J. A. Small-molecule inhibitors of protein-protein interactions: Progressing towards the dream. *Nat. Rev. Drug Discovery* **2004**, *3*, 301−317.

(6) Caffrey, D. R.; Somaroo, S.; Hughes, J. D.; Mintseris, J.; Huang, E. S. Are protein-protein interfaces more conserved in sequence than the rest of the protein surface? *Protein Sci.* **2004**, *13*, 190−202.

(7) Veselovsky, A. V.; Archakov, A. I. Inhibitors of Protein-Protein Interactions as Potential Drugs. *Curr. Comput.-Aided Drug Des.* **2007**, *3*, 51−58.

(8) Wells, J. A.; McClendon, C. L. Reaching for high-hanging fruit in drug discovery at protein-protein interfaces. *Nature* **2007**, *450*, 1001−1009.

(9) Van Maele, B.; Busschots, K.; Vandekerckhove, L.; Christ, F.; Debyser, Z. Cellular co-factors of HIV-1 integration. *Trends Biochem. Sci.* **2006**, *31*, 98−105.

(10) Cherepanov, P.; Maertens, G.; Proost, P.; Devreese, B.; Van Beeumen, J.; Engelborghs, Y.; De Clercq, E. Debyser, Z. HIV-1 integrase forms stable tetramers and associates with LEDGF/p75 protein in human cells. *J. Biol. Chem.* **2003**, *278*, 372−381.

(11) Ciuffi, A.; Llano, M.; Poeschla, E.; Hoffmann, C.; Leipzig, J.; Shinn, P.; Ecker, J. R.; Bushman, F. A role for LEDGF/p75 in targeting HIV DNA integration. *Nat. Med.* **2005**, *11*, 1287−1289.

(12) Llano, M.; Saenz, D. T.; Meehan, A.; Wongthida, P.; Peretz, M.; Walker, W. H.; Teo, W. L.; Poeschla, E. M. An essential role for LEDGF/p75 in HIV integration. *Science* **2006**, *314*, 461−464.

(13) Ciuffi, A.; Bushman, F. D. Retroviral DNA integration: HIV and the role of LEDGF/p75. *Trends Genet.* **2006**, *22*, 388−395.

(14) Al-Mawsawi, L. Q.; Neamati, N. Blocking interactions between HIV-1 integrase and cellular cofactors: an emerging anti-retroviral strategy. *Trends Pharmacol. Sci.* **2007**, *28*, 526−535.

(15) Poeschla, E. M. Integrase, LEDGF/p75 and HIV replication. *Cell. Mol. Life Sci.* **2008**, *65*, 1403−1424.

(16) De Rijck, J.; Vandekerckhove, L.; Gijsbers, R.; Hombrouck, A.; Hendrix, J.; Vercammen, J.; Engelborghs, Y.; Christ, F.; Debyser, Z. Overexpression of the lens epithelium-derived growth factor/p75 integrase binding domain inhibits human immunodeficiency virus replication. *J. Virol.* **2006**, *80*, 11498−11509.

(17) Hombrouck, A.; De Rijck, J.; Hendrix, J.; Vandekerckhove, L.; Voet, A.; De Maeyer, M.; Witvrouw, M.; Engelborghs, Y.; Christ, F.; Gijsbers, R.; Debyser, Z. Virus evolution reveals an exclusive role for LEDGF/p75 in chromosomal tethering of HIV. *PLoS Pathog.* **2007**, *3*, e47.

(18) Du, L.; Zhao, Y. X.; Chen, J.; Yang, L. M.; Zheng, Y. T.; Tang, Y.; Shen, X.; Jiang, H. L. D77, one benzoic acid derivative, functions as

a novel anti-HIV-1 inhibitor targeting the interaction between integrase and cellular LEDGF/p75. *Biochem. Biophys. Res. Commun.* **2008**, *375*, 139−144.
(19) De Luca, L.; Barreca, M. L.; Ferro, S.; Christ, F.; Iraci, N.; Gitto, R.; Monforte, A. M.; Debyser, Z.; Chimirri, A. Pharmacophore-Based Discovery of Small-Molecule Inhibitors of Protein-Protein Interactions between HIV-1 Integrase and Cellular Cofactor LEDGF/p75. *ChemMedChem* **2009**, *4*, 1311−1316.
(20) De Luca, L.; Ferro, S.; Gitto, R.; Barreca, M. L.; Agnello, S.; Christ, F.; Debyser, Z.; Chimirri, A. Small molecules targeting the interaction between HIV-1 integrase and LEDGF/p75 cofactor. *Bioorg. Med. Chem.* **2010**, *18*, 7515−7521.
(21) Christ, F.; Voet, A.; Marchand, A.; Nicolet, S.; Desimmie, B. A.; Marchand, D.; Bardiot, D.; Van der Veken, N. J.; Van Remoortel, B.; Strelkov, S. V.; De Maeyer, M.; Chaltin, P.; Debyser, Z. Rational design of small-molecule inhibitors of the LEDGF/p75-integrase interaction and HIV replication. *Nat. Chem. Biol.* **2010**, *6*, 442−448.
(22) Tsiang, M.; Jones, G. S.; Niedziela-Majka, A.; Kan, E.; Lansdon, E. B.; Huang, W.; Hung, M.; Samuel, D.; Novikov, N.; Xu, Y.; Mitchell, M.; Guo, H.; Babaoglu, K.; Liu, X.; Geleziunas, R.; Sakowicz, R. New class of HIV-1 integrase (IN) inhibitors with a dual mode of action. *J. Biol. Chem.* **2012**, *287*, 21189−21203.
(23) Christ, F.; Shaw, S.; Demeulemeester, J.; Desimmie, B. A.; Marchand, A.; Butler, S.; Smets, W.; Chaltin, P.; Westby, M.; Debyser, Z.; Pickford, C. Small-molecule inhibitors of the LEDGF/p75 binding site of integrase block HIV replication and modulate integrase multimerization. *Antimicrob. Agents Chemother.* **2012**, *56*, 4365−4374.
(24) Harvey, A. L. Natural products in drug discovery. *Drug Discovery Today* **2008**, *13*, 894−901.
(25) Bissantz, C.; Folkers, G.; Rognan, D. Protein-based virtual screening of chemical databases. 1. Evaluation of different docking/scoring combinations. *J. Med. Chem.* **2000**, *43*, 4759−4767.
(26) Jahn, A.; Hinselmann, G.; Fechner, N.; Zell, A. Optimal assignment methods for ligand-based virtual screening. *J. Cheminform.* **2009**, *1*, 14.
(27) Hou, Y.; McGuinness, D. E.; Prongay, A. J.; Feld, B.; Ingravallo, P.; Ogert, R. A.; Lunn, C. A.; Howe, J. A. Screening for antiviral inhibitors of the HIV integrase - LEDGF/p75 interaction using the AlphaScreen (TM) luminescent proximity assay. *J. Biomol. Screening* **2008**, *13*, 406−414.
(28) *QikProp*, version 3.4, Schrödinger, LLC, New York, NY, 2011.
(29) Cherepanov, P.; Ambrosio, A. L. B.; Rahman, S.; Ellenberger, T.; Engelman, A. Structural basis for the recognition between HIV-1 integrase and transcriptional coactivator p75. *Proc. Natl. Acad. Sci. U.S.A.* **2005**, *102*, 17308−17313.
(30) Busschots, K.; Voet, A.; De Maeyer, M.; Rain, J. C.; Emiliani, S.; Benarous, R.; Desender, L.; Debyser, Z.; Christ, F. Identification of the LEDGF/p75 binding site in HIV-1 integrase. *J. Mol. Biol.* **2007**, *365*, 1480−1492.
(31) *Prime*, version 2.1, Schrödinger, LLC, New York, NY, 2009.
(32) *Glide*, version 5.5, Schrödinger, LLC, New York, NY, 2009.
(33) *LigPrep*, version 2.3, Schrödinger, LLC, New York, NY, 2009.
(34) Friesner, R. A.; Banks, J. L.; Murphy, R. B.; Halgren, T. A.; Klicic, J. J.; Mainz, D. T.; Repasky, M. P.; Knoll, E. H.; Shelley, M.; Perry, J. K.; Shaw, D. E.; Francis, P.; Shenkin, P. S. Glide: a new approach for rapid, accurate docking and scoring. 1. Method and assessment of docking accuracy. *J. Med. Chem.* **2004**, *47*, 1739−1749.
(35) Brooijmans, N.; Humblet, C. Chemical space sampling by different scoring functions and crystal structures. *J. Comput.-Aided Mol. Des.* **2010**, *24*, 433−447.
(36) Zhang, Y. N.; Zhang, W.; Hong, D.; Shi, L.; Shen, Q.; Li, J. Y.; Li, J.; Hu, L. H. Oleanolic acid and its derivatives: new inhibitor of protein tyrosine phosphatase 1B with cellular activities. *Bioorg. Med. Chem.* **2008**, *16*, 8697−8705.
(37) Ma, L.; Yang, Z.; Li, C.; Zhu, Z.; Shen, X.; Hu, L. Design, synthesis and SAR study of hydroxychalcone inhibitors of human beta-secretase (BACE1). *J. Enzyme Inhib. Med. Chem.* **2011**, *26*, 643−648.
(38) Jenkins, T. M.; Engelman, A.; Ghirlando, R.; Craigie, R. A soluble active mutant of HIV-1 integrase: involvement of both the core and carboxyl-terminal domains in multimerization. *J. Biol. Chem.* **1996**, *271*, 7712−7718.
(39) Zheng, Y. T.; Zhang, W. F.; Ben, K. L.; Wang, J. H. In vitro immunotoxicity and cytotoxicity of trichosanthin against human normal immunocytes and leukemia-lymphoma cells. *Immunopharmacol. Immunotoxicol.* **1995**, *17*, 69−79.